



## Growth and characterization of dipotassium sodium tetraborate octahydrate

### $K_2Na[B_4O_5(OH)_4]_2 \cdot 8H_2O$ : A potential non linear optical single crystals

V.Krishnakumar<sup>1</sup>, S.Sivakumar<sup>2</sup>, R.Nagalakshmi<sup>3</sup> and Ivan V.Kityk<sup>4</sup>

<sup>1</sup>Department of Physics, Periyar University, Salem – 636 011, India.

<sup>2</sup>Department of Physics, Arignar Anna Government Arts College, Attur-636 121, India.

<sup>3</sup>Department of Physics, National Institute of Technology, Trichy- 620 015, India.

<sup>4</sup>Department of Chemistry, Silesian University of Technology, Poland.

#### ARTICLE INFO

##### Article history:

Received: 25 January 2011;

Received in revised form:

20 February 2011;

Accepted: 26 February 2011;

##### Keywords

DFT calculations

Vibrational analysis;

Infrared and Raman spectra.

#### ABSTRACT

Dipotassium sodium tetraborate octahydrate-  $K_2Na[B_4O_5(OH)_4]_2 \cdot 8H_2O$  (KNB) is an intriguing crystal for laser frequency conversion. It was grown by slow evaporation solution growth technique at ambient temperature. The investigated crystal is crystallized into noncentrosymmetric orthorhombic axial  $P2_12_12_1$  space group. Fundamental optical phonon modes were identified and the assignments were proposed. The dependence of second order optical susceptibilities with the applied d.c field strength for two principal geometries was studied. Piezooptical coefficients for the diagonal  $P_{xxxx}$  and off-diagonal  $P_{xxzz}$  tensor components under applied dc-field also were measured and discussed. Correlation between the anisotropy of the obtained spectra and of the observed nonlinear optical susceptibilities was established.

© 2011 Elixir All rights reserved.

#### Introduction

Inorganic borate crystals find widespread application as nonlinear promising optical materials in high performance devices. Till now researchers have synthesized several new materials and achieved advances both in materials processing and in device engineering physics that will likely lead to a broader application. Due to the possibility of wide isomorphous substitutions one can consider these borates as polyfunctional materials with device potential laser and non-linear optical materials with high efficiency, new laser medium with double function and tunability, piezoelectrics and acousto electrics etc. Borates have the outstanding characteristics for frequency conversion into UV. Most of the borate crystals contain independent orthoborate  $BO_3$  groups in their structures. The collective existence of these properties in individual compounds has resulted in several unique performance characteristics that include generation of coherent light to wavelengths below 200 nm and the production of continuously tunable, high-power coherent radiation from 350-2400 nm spectral wavelength. To date, many of the achievements in borate crystals have been made possible by the improvements both in the growth of good quality of non-linear optical crystals and in laser-source performance. Since boron atoms can form planar or non-planar  $BO_3$  groups, where the oxygen atoms form  $B(sp^2)$ -O bonds and also tetrahedral  $BO_4$  groups where four oxygen atoms form  $B(sp^3)$ -O bonds, the borate compounds present a great structural complexity which makes borate crystal exhibit interesting physical properties. The isolated  $[B_4O_5(OH)_4]^{2-}$  has been found in lot of hydrated borates. The structure of six hydrated mixed borates containing alkaline and alkaline earth metal cations [1-3] has been established. Motivated by these properties of borate based materials and in continuation of attempt of growing non linear optical crystals, this paper presented the crystal growth and characterization of the hydrated mixed borate  $K_2Na[B_4O_5(OH)_4]_2 \cdot 8H_2O$  an inorganic non linear optical single crystal, also measured the field induced second harmonic

generation, piezooptics effect of the investigated crystal and discussed the results.

#### Experimental Techniques

##### Synthesis and Crystal growth

KNB was synthesized from  $K_2CO_3$ ,  $H_3BO_3$  and NaCl. The calculated amount of the reactants were thoroughly dissolved in double distilled water and heated water. After  $CO_2$  release, the above solution was mixed with NaCl to form an amorphous precipitate. The mixture was stirred well for two hours to yield a homogeneous mixture at  $75^\circ C$ . To prevent possible decomposition, the colourless crystalline sample of the title compound was obtained and recrystallized several times before starting the growth process. Borate solutions are usually viscous. It takes longer time to evaporate.

The solubility of the studied compound was assessed in different solvents apart from deionized water. But the investigated crystal was found to have good solubility in deionized water. The solubility of KNB was evaluated as a function of temperature in the temperature range  $30^\circ C$  to  $60^\circ C$ . A thermostatically controlled vessel was filled with the solution of the title compound and with some undissolved KNB and stirred for a day. The next day a small amount of the supernatant solution was pipetted out and the concentration of the solute was determined gravimetrically. Fig.1 shows the solubility curve of the studied compound. The solubility studies reveal that the investigated compound exhibits good solubility and a positive solubility temperature gradient in deionized water. Single crystals have been grown from saturated solution at a pH of 3.5 by slow evaporation solution growth technique at  $35^\circ C$  using constant temperature bath having controlled accuracy of  $0.01^\circ C$ . The crystals with perfect shape and transparency were formed by spontaneous nucleation in the supersaturated solution. The crystallization begins in a few days. The growth of the title compound needed a more than a month. Single crystals with good optical quality in regular shape with dimensions of  $6 \times 5 \times 4 \text{ mm}^3$  have been obtained. The photograph of the grown crystals is depicted in Fig.2.

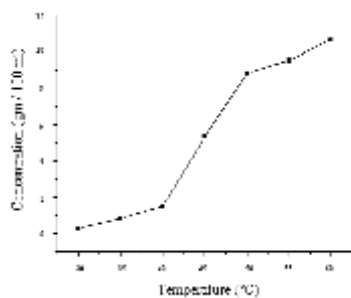


Fig.1 Solubility curve of KNB



Fig. 2 Photograph of the KNB crystal grown in water

#### Recording of spectra

#### X-ray diffraction studies

The structural properties of  $K_2Na[B_4O_5(OH)_4]_2 \cdot 8H_2O$  (KNB) have been studied by X-Ray powder diffraction technique. The X-Ray diffraction studies were carried out using SEIFERT diffractometer with  $CuK\alpha_1$  ( $\lambda = 1.5406 \text{ \AA}$ ) radiation. From the powdered X-ray data, the various planes of reflections were indexed using XRDA 3.1 program and the lattice parameters were evaluated. The indexed X-ray diffraction pattern and the morphology are shown in Fig.3(a) and 3(b) respectively. The XRD data confirms that the crystal is orthorhombic with the space group  $P2_12_12_1$ , a well-known non-centrosymmetric space group thus satisfying the requirements for second order NLO activity. The unit cell is found to be tetra molecular. The crystallographic data is given in Table.1. It has been observed that  $P2_12_12_1$  is one among the popular space group and it allows maximal contribution of the molecular nonlinearity to the macroscopic crystal nonlinearity. It consists of discrete  $B_4O_5(OH)_4^{2-}$  borate anions separated by isolated water molecules and  $Na^{2+}$  and  $K^+$  ions. The dipole moment of the crystal is large, which influences the essential nonlinear optical properties such as second harmonic generation (SHG) efficiency etc.

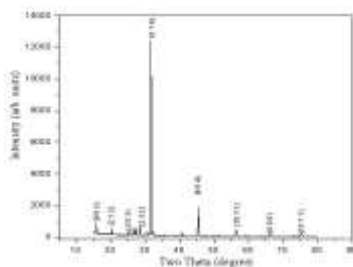


Fig. 3(a) The indexed X-ray diffraction pattern of KNB

#### Recording of Phonon Spectra

The room temperature mid Fourier transform infrared spectrum of KNB shown in Fig.4 was recorded in the spectral range  $400-4000\text{cm}^{-1}$  at a resolution of  $4\text{cm}^{-1}$  using Perkin Elmer Fourier transform Infrared Spectrophotometer, model SPECTRUM RX1, using KBr pellets containing a fine powder of the title compound obtained from the grown single crystals, equipped with a  $LiTaO_3$  detector, a KBr beam splitter, He-Ne Laser source and boxcar apodization used for 250 averaged

interferogrammes collected for both the sample and the background.

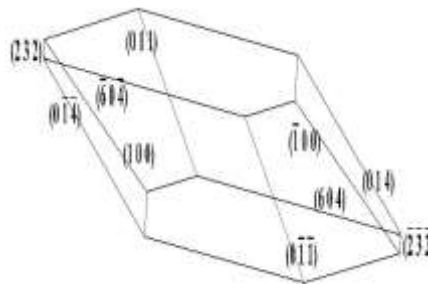


Fig. 3(b) Morphology of KNB

Identification code	KNB
Empirical formula	$K_2Na[B_4O_5(OH)_4]_2 \cdot 8H_2O$
Colour and shape	White, prismatic
Crystal structure	Orthorhombic
Space group	$P2_12_12_1$
Cell parameters	
a( $\text{\AA}$ )	16.597
b( $\text{\AA}$ )	12.469
c( $\text{\AA}$ )	11.569
$\alpha$ ( $^\circ$ )	90
$\beta$ ( $^\circ$ )	90
$\gamma$ ( $^\circ$ )	90
Volume ( $\text{\AA}^3$ )	2394.2
Z	4
Crystal size	$6 \times 5 \times 4 \text{ mm}^3$
UV cut off wavelength	190 nm
Band gap	6.03 eV

Table 1

#### Crystallographic data of KNB

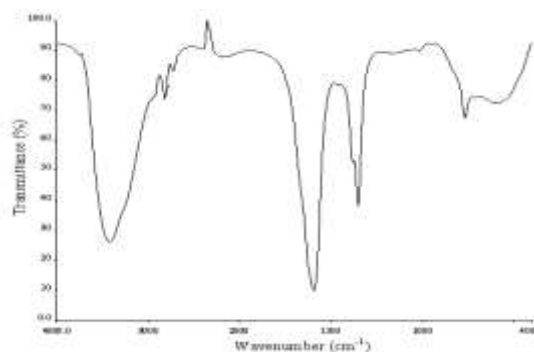


Fig. 4 Experimental FT IR spectrum of KNB

The FT Raman spectrum was recorded on a BRUKER IFS 66V model interferometer equipped with an FRA-106 FT Raman accessory. The observed spectra given in Fig.5(a) and 5(b) were recorded in the  $3500 - 100 \text{ cm}^{-1}$  Stokes region using the 514 nm line of argon ion laser for excitation operating at 80 mW power. The reported wave numbers are believed to be reproduced within  $1 \text{ cm}^{-1}$ .

#### Dielectric Measurements

Studies of the temperature and frequency dependence of dielectric properties can unveil useful information about structural changes, defect behavior and transport phenomena [4]. Good samples of KNB crystals were polished on a soft tissue paper with fine grade alumina powder ( $0.1\mu\text{m}$ ) dispersed in a mixture of methanol and dimethyl sulphoxide in the volume ratio 1:4. Each sample was electroded on either side with silver paste (air drying) to make it behave like a parallel plate capacitor.

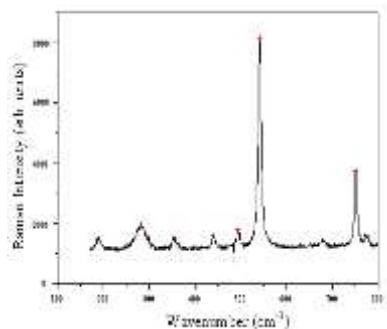


Fig. 5(a) FT Raman spectrum of KNB (medium wavenumber region)

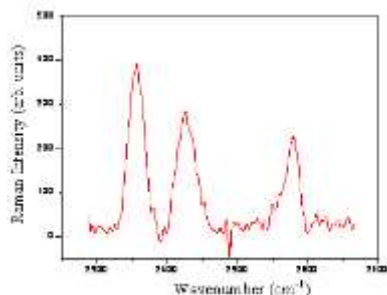


Fig. 5(b) FT Raman spectrum of KNB (higher wavenumber region)

Typical sample thickness is about 3.69 mm. A HIOKI (model 3535) LCR meter was used to measure capacitance,  $\tan \delta$ , dc conductivity of the sample as a function of frequency and temperature (in the range 35–85°C). A small rectangular furnace of 20 x 20 x 20 cm<sup>3</sup> dimensions whose temperature was controlled by a Eurotherm controller (0.1°C) was used to house the sample. The dielectric constant was calculated using the relation:

$$\epsilon_r = \frac{Ct}{\epsilon_0 A}$$

where  $\epsilon_0$  is the permittivity of free space,  $t$  is the thickness of the sample, and  $A$  is the area of cross section of the sample. The setup was calibrated using the standard material BaTiO<sub>3</sub>.

## Results and Discussions

### Structural Analysis

The structure of the studied crystal consists of alternate layers of tetraborate anions, cations and water molecules. Two [B<sub>4</sub>O<sub>5</sub>(OH)<sub>4</sub>]<sup>2-</sup> are located on different infinite layers and are linked by electrostatic and hydrogen bonds. From crystallographic point of view, K<sub>2</sub>Na[B<sub>4</sub>O<sub>5</sub>(OH)<sub>4</sub>]<sub>2</sub>·8H<sub>2</sub>O containing the borate polyanion B<sub>4</sub>O<sub>5</sub>(OH)<sub>4</sub> is constituted of two BO<sub>2</sub>(OH) groups (triangular) and two BO<sub>2</sub>(OH) groups (tetrahedral).

The two [B<sub>4</sub>O<sub>5</sub>(OH)<sub>4</sub>]<sup>2-</sup> clusters are linked by K<sup>+</sup> through K-O to form a three dimensional structures which are linked by electrostatic forces and hydrogen bonds. The crystallographic structures of these borates consist predominantly of the boron-oxygen network throughout the crystal.

All the principal features of the borate crystals are determined mainly by the network. The observed wavenumbers, relative intensities obtained from the recorded spectra and the assignments proposed for the title nonlinear optical crystal is given in Table.2.

### Description of Phonon modes

Analysis of Raman and infrared phonon modes are helpful to understand the various bonding properties of the crystalline materials existing in the condensed state.

Table 2  
Observed FT IR and FT Raman wavenumbers (in cm<sup>-1</sup>) of KNB and its vibrational assignments

Wavenumbers FT Raman	Wavenumbers FT IR	Assignments
3580 s	-	$\nu_{as}(\text{O-H})$
3426 s	-	$\nu_{as}(\text{O-H})$
3357 s	-	$\nu_s(\text{O-H})$
-	1595 s	$\delta(\text{H-O-H})$
-	1353 s	$\delta_{in\ plane}(\text{B-OH})$
-	1019 w	$\nu_{as}(\text{B-O})$
903 ms	-	$\nu_{as}(\text{B-O})$
750 s	-	$\nu_s(\text{B-O})$ and $\delta(\text{B-O})$
-	-	$\delta_{as}(\text{OBO})$ ring
677 w	-	$\delta_{as}(\text{OBO})$ ring
540 s	-	$\phi[\text{B}_4\text{O}_5(\text{OH})_4]^{2-}$
493 m	-	$\phi[\text{B}_4\text{O}_5(\text{OH})_4]^{2-}$
438 m	-	OBO terminal bending
354 m	-	$\delta(\text{OBO})$
281 ms	-	Lattice vibrations of metal ions

$\nu_{as}$ , asymmetric stretching;  $\nu_s$ , symmetric stretching;  $\delta$ , deformation;  $\phi$ , ring; w, weak; m, medium; ms, medium strong; s, strong;

The IR spectra of this compound exhibit bands in the region 3000–3500 cm<sup>-1</sup> due to stretching vibrations of OH groups and water molecules which are involved in the hydrogen bondings. The middle band at 1595 cm<sup>-1</sup> is related to H-O-H bending mode. In the borate compounds containing (BO<sub>3</sub>)<sup>3-</sup> groups, the electronic delocalization in the planar borate anion is predominant and hence induces NLO properties (linked to their polarizability) as well as large birefringence (depending upon the relative orientation of the borate groups) required to fulfill the phase matching conditions [5]. Also the boron atom has a non-bonded pair of electron and hence the molecules or ions of the form (BO<sub>x</sub>)<sup>n-</sup> are suitable building blocks for preparing acentric (non-centrosymmetric) crystals, which are required for generating nonlinear optical properties. The absorption bands at in the range of 1500–500 cm<sup>-1</sup> might be considered as the characteristic peak of polyborate anions. Again, the strong bands at about 1353 cm<sup>-1</sup> of IR are consistent with the existence of trigonally coordinated boron, the bands near 905 cm<sup>-1</sup> are characteristic of tetrahedral boron. A complete study of IR spectra of hydrated borates were carried out by Moneke [6,7], Weir [8] and Valyashko [9,10]. In the spectral region below 600 cm<sup>-1</sup>, BO<sub>3</sub> bending phonons are expected. Strong bands at 1019 cm<sup>-1</sup> can be assigned to stretching vibrations of B<sub>4</sub>-O, whereas the bending vibration of B<sub>4</sub>-O occurs at 493 cm<sup>-1</sup>. The Raman optical phonon modes at 1353 and 903 cm<sup>-1</sup> can be caused by asymmetric and symmetric stretching vibration of B<sub>3</sub>-O. The two spectrally middle bands at 750 and 677 cm<sup>-1</sup> in Raman phonon spectra and 769 and 603 cm<sup>-1</sup> in IR are attributed to bending mode of B<sub>3</sub>-O. Janda and Heller [11] have studied the IR and Raman spectra of tetra borates and pentaborate with boron isotope substitution. Based on their study a middle sharp intense band observed at 540 cm<sup>-1</sup> is attributed to the vibration of tetra borate B<sub>4</sub>O<sub>5</sub>(OH)<sub>4</sub>. All the compounds containing basic B<sub>4</sub>O<sub>5</sub>(OH)<sub>4</sub> anion with different degrees of hydration and polymerization show similar spectra [8,12]. We recorded single crystal Raman phonon spectra for two random orientations and we could see substantial intensity variations. The variation in intensity can be explained due to a competition between the long-range electrostatic forces (polar forces) and short-range

molecular forces (anisotropic lattice forces) prevail in the piezoelectric borate crystals.

### Dielectric Behaviour

In the investigated crystal the capacitance decreases with increasing frequency as shown in Fig. 6(a). This effect can be explained by charge distribution by mean carrier hopping on defects. At low frequency, the charge on the defects can be rapidly redistributed so that defects closer to the positive side of the applied field become negatively charged, while defects closer to the negative side of the applied field become positively charged. This leads to a screening of the field and an overall reduction in the electric field. Because capacitance is inversely proportional to the field, this reduction in the field for a given voltage results in the increased capacitance observed as the frequency is lowered. At high frequencies, the defects no longer have enough time to rearrange in response to the applied voltage, hence the capacitance decreases [13,14].

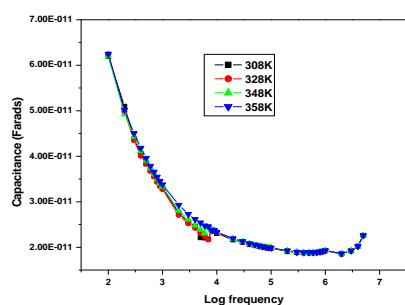


**Fig. 6(a) Variation of capacitance with frequency**

The dielectric behavior of borates arises mainly from ionic motions. The free energy barriers impeding the ionic diffusion are expected to vary from site to site in glassy semiconductors, so there are different ionic motions in such glasses. The first is the rotation of ions around their negative sites. The second is the hopping of ions from sites with low free energy up to sites with high free energy in the direction of electric field or slowly oscillates between the sites with high free energy in a fast alternating electric field. Both the first and the second motions give a significant contribution to the dielectric constant.

The variation in dielectric constant with frequency is shown in Fig.6(b). It is observed that the dielectric constant decreases ceaselessly with increase in frequency succeeded with a frequency independent behavior at high frequencies (from 90 kHz up to 5 MHz). The large values of dielectric constant at low frequency enumerates that there is a contribution from all four known sources of polarization namely, electronic, ionic, dipolar and space charge polarization. Space charge polarization is generally active at lower frequencies and high temperatures and betokens the perfection of the crystals [15]. Further, the space charge polarization will reckon on the purity and perfection of the material. Its influence is large at higher temperature and is noticeable in the low frequency region [16]. From Fig. 6(b), it is understood that the thermal activation on charge carriers is negligible i.e., the variation of dielectric constant with varying temperature is very meager or negligible. This suggests that the sample possess high chemical homogeneity [17].

### Optical Transmission Spectrum

The optical property of the material gives information regarding the composition nature and the quality of the crystal. The present experimental study may be assisted in understanding electronic structure of the electronic optical band gap of KNB. The transparency of KNB crystal was measured using Perkin Elmer Lambda 35 UV visible spectrophotometer

in the spectral range 190 to 1100 nm and the transmittance spectrum of the pure crystal is shown in the Fig. 7(a).

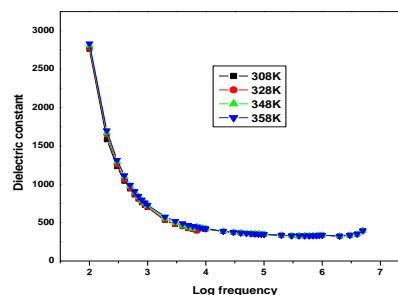


**Fig. 6(b) Variation of dielectric constant with frequency**

From the recorded UV spectra it is evident that the KNB displays an excellent transmission in the entire UV-Vis region. The study of the absorption edge is essential in connection with the theory of electronic structure, which leads to the prediction of whether the band structure is affected near the band extreme. So the main goal was to determine the magnitude and the nature of optical energy band gap of KNB crystal.

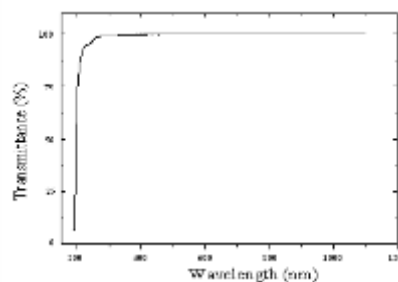


**Fig. 7(a) Optical transmission spectrum of KNB**

An increase in transmittance exists near 190 nm of the optical transmission spectrum. Fig. 7(b) shows the plot of  $(ahv)^2$  against photon energy  $hv$  for the KNB crystal. The extrapolation of the curve to zero  $(ahv)^2$  shows its direct band gap type around 6.03 eV. Since the crystal is wide energy band it possesses large transmittance in the visible region. The energy gaps of semiconductors are much smaller than those of the borate crystals. Also there were very little absorptions at the doubled (532 nm) and tripled (355 nm) wavelengths. The nonlinear optical properties of crystals are linked to crystal structure, in particular to the presence of certain molecular ions [18]. For borate family crystals, theoretical analysis showed that the B-O rings are ideal basic structure units for new ultra violet nonlinear optical crystals. Allowing for orbit hybridization, the ultraviolet cutoff wavelength of borate crystals depends on  $\pi - \pi^*$  transitions of planar B-O rings [19,20]. This results in the shortening of UV absorption edge below 200 nm in the recorded spectrum of KNB. Thus the important and interesting application of the mentioned crystals may be connected with its highly anisotropic optical properties in the blue spectral region. This is necessary for creation of polarised optical filters, passive laser Q-switchers and beam-splitter for the blue laser.

### Second order nonlinear susceptibility and Piezooptical studies

For many applications, no convenient source exists for the direct production of laser light having the proper frequency and power characteristics. For these uses requisite frequency and power may be generated passing a laser beam through a suitable nonlinear optical crystal. To confirm this, second harmonic generation (SHG) measurements were performed on crushed crystals using a modified Kurtz-Perry NLO system with a 1064 nm fundamental laser light source.

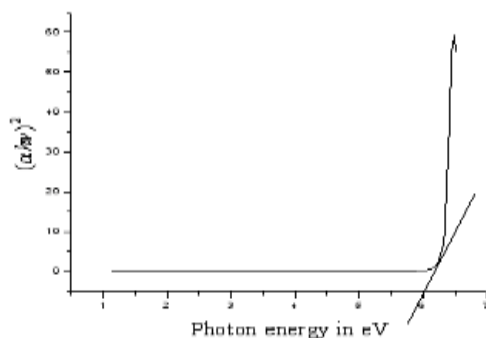


Fig. 7(b) Plot of  $(\alpha hv)^2$  versus photon energy  $hv$

The second-harmonic signal at 532 nm was clearly observed for  $K_2Na[B_4O_5(OH)_4]_2 \cdot 8H_2O$  supporting the assignment of this structure in a non-centrosymmetric setting. The relative second harmonic efficiency of the KNB crystal is found to be 12 mV for the input power of 5.7 mJ/pulse when compared to that of standard KDP (16 mV). Because of their robust characteristics and wide SHG transparency ranges, borates have become preferred NLO crystals for applications with frequency requirements have extended from the deep UV to the near IR.

The description of observed Raman optical phonon modes reveals that the investigated crystal possess high anisotropy of chemical bonds and this favours the substantial anisotropy in second order nonlinear optical susceptibility of KNB. Moreover, it reflects the layered structural architecture of particular borate clusters. In order to explore the manifestations of the anisotropy we have performed the measurements of the SHG for the two principal geometry. The first one corresponds to the S-S (input-output SHG geometry) and the second one corresponds to the S-P geometry. It is important that the second order optical susceptibility for the S-P geometry is almost two times larger than that of S-S. This observed experimental feature is due to the interlayer charge transfer of ions in the KNB, which is in agreement with the Raman spectral analysis. At the same time the mentioned structural and Raman data also indicate on existence a large number of the inter-layer voids. The additional alignment of the particular clusters in the investigated crystal may be achieved by applying of dc-electric field. We have done the measurements of the SHG in the presence of applied electric field and we have evaluated the values of the corresponding second order optical susceptibilities following the reference crystals, like  $KTiOPO_4$ . In the Fig.8 we have presented the corresponding field-induced dependences of the SHG. From Fig. 8, one can see that for the S-S polarization. We have achieved additional growth of second order susceptibility values (upto 0.85 pm/V) at dc electric strength about 850 V/cm. At the same time for the S- P polarization the corresponding output second order susceptibility decreases achieving the value about 1 pm/V. For the electric strength about the 900 V/cm the corresponding values of the second order susceptibilities were saturated on the levels about 1 pm/V and 0.82 pm/V for the S-P and S-S SHG geometries, respectively. The finger print regions of the optical phonon spectra of the investigated crystal suggest that the substantial contributions of electron-phonon interactions are possible in the crystal lattice of borate crystals. The electron-phonon interactions play a prevailing and substantial role on the piezooptical coefficients [21]. To verify this in the investigated crystal, we have performed measurements of the piezooptical coefficients for the diagonal  $P_{xxxx}$  and off-diagonal  $P_{xxzz}$  tensor components.

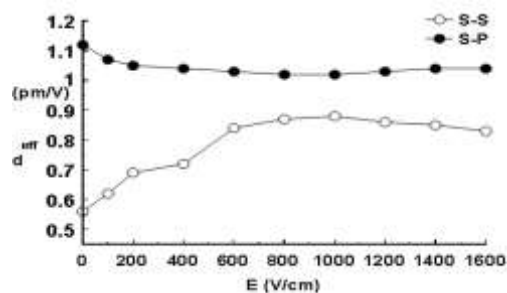


Fig. 8 dc-field dependence of the second order susceptibilities

The corresponding measurements were done using the Senarmont method to determine the field induced birefringence [22] (with precisions up to  $10^{-5}$ ), which allow to evaluate the piezooptical coefficients with accuracy up to  $3 \times 10^{-15} \text{ m}^2/\text{N}$ . Similarly to the anisotropic SHG the corresponding piezooptical coefficients demonstrate larger piezooptics for the off-diagonal terms (about  $6.2 \times 10^{-14} \text{ m}^2/\text{N}$ ) compared to diagonal components ( $3.4 \times 10^{-14} \text{ m}^2/\text{N}$ ) at He-Ne laser wavelength (Fig. 9). The applied dc electric field demonstrates the features similar to the previous case (Fig. 8).

The observed measurements confirm that the diagonal piezooptical tensor components are enhanced and non-diagonal ones are decreased. The difference with respect to the SHG consists that the corresponding piezooptical extrema achieve their maxima at electric strengths about 570 V/cm, which are substantially lower compared to the 900 V/cm for the optical SHG (compared Fig.8 and Fig. 9). It may indicate that the principal mechanisms of these two methods are principally different in the external electric fields. In the case of SHG the electron-phonon interactions is determined by lower energy phonons whereas in the case of the piezooptics the situation is otherwise. Moreover, in piezooptical measurements we do not observe the dc-field dependent saturational processes like for the SHG.

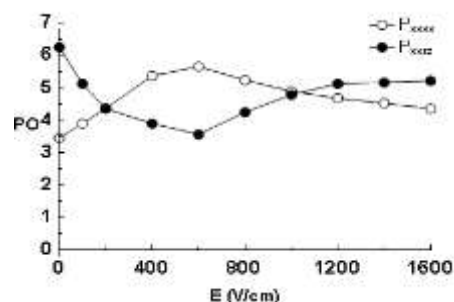


Fig.9 Dependence of the diagonal and off-diagonal piezooptical coefficients

## Conclusion

Single crystals with good optical quality of dimensions of  $6 \times 5 \times 4 \text{ mm}^3$  obtained from aqueous solution by slow evaporation technique at room temperature were characterized. The XRD data confirms that the crystal is orthorhombic in structure with the space group  $P2_12_12_1$ , a well-known non-centrosymmetric space group thus satisfying the requirements for second order NLO activity.

The observed optical phonon modes were assigned unambiguously. The variations in the intensities were observed in the Raman phonon spectra. This is due to the presence of long-range electrostatic forces (polar forces) and short-range molecular forces (anisotropic lattice forces) prevail in the piezoelectric borate crystals. From the results of optical transmission it was found that the crystal exhibit excellent transmission in entire UV-Vis range studied.

The calculated wide electronic bandgap (6.03eV) enables the KNB for large transmittance in the visible region. The effect of charge distribution by mean carrier hopping on defects in the investigated crystal results in the decrease of capacitance with increasing frequency. The results of Kurtz powder experiments of KNB confirmed that the relative second harmonic efficiency is comparable to that of KDP. In addition, the results of the measurements of the second harmonic generation for the two principal geometry of KNB crystal showed that the second order optical susceptibility varies drastically with respect to the geometry of the crystal and the strength of the applied field. This behaviour observed could be due to the inter layer charge transfer of ions in the crystal. Similarly to the anisotropic SHG the corresponding piezooptical coefficients demonstrate larger piezooptics for the off-diagonal terms (about  $6.2 \times 10^{-14} \text{ m}^2/\text{N}$ ) compared to diagonal components ( $3.4 \times 10^{-14} \text{ m}^2/\text{N}$ ). The difference with respect to the SHG consists that the corresponding piezooptical extrema achieve their maxima at electric strengths about 570 V/cm, which are substantially lower compared to the 900 V/cm for the optical SHG, which may indicate that the principal mechanisms of these two methods are principally different in the external electric fields.

#### References

- 1.A.Ben Ali, L.S.Simiri, V.Maisonneuve, *J.Alloys compd.*, 322 (2001) 153.
- 2.N.P.Ivenchko, E.N.Kurkutova, *Kristallographia.*, 20 (1975) 33.
- 3.X.Solans, J.Solans, M.V.Domenech, *Acta. Crystallogr.*, C53 (1997) 994.
- 4.H.M.Lin, Y.F.Chen, J.L.Shen, W.C.Chou, *J.App.Phys.*, 89 (2001) 4476.
- 5.C.T. Chen in: *Development of New Nonlinear Optical Crystals in the Borate Series Laser Science and Technology*, Harwood Academic, Switzerland, 1993
- 6.H.Moenke, *Mineralspekren I*, Akademie, Berlin, 1962.
- 7.H.Moenke, *Mineralspekren II*, Akademie, Berlin, 1966.
- 8.C.E.Weir, *J. Res. Nat. Bur.Stand.*, 70A (1966) 153.
- 9.E.V.Wlassowa, M.G.Valyashko, *Russ J. Inorg. Chem.*, 11 (1966) 1539.
- 10.M.G.Valyashko, E.V.Wlassowa, *Jena Rev.*, 14 (1969) 3.
- 11.R.Janda, G.Heller, *Spectrochim. Acta.*, 36A (1980) 997.
- 12.J.Li, Sh.P.Xia, Sh.Y.Gao, *Spectrochim. Acta.*, 51A (1995) 519.
- 13.P.W.Zukowski, S.B.Kantorow, D.Maczka, V.F.Stelmakh, *Phys.Status Solidi A.*, 112 (1989) 695
- 14.A.Vasudevan, S.Carín, M.R.Melloch, S.Hannon, *Appl. Phys. Lett.*, 73 (1998) 671.
- 15.N.V.Prasad, G.Prasad, T.Bhimasankaran, S.V.Suryanarayan, G.S.Kumar, *Indian J.Pure & Appl Phy.*, 34 (5) (1996) 639.
- 16.C.P.Smyth, *Dielectric behavior and structure*, Mc Graw Hill, New York, 1955.
- 17.J.Benet Charles, F.D.Gnanam, *Cryst.Res.Tech.*, 29 (1994) 707.
- 18.J.F.H. Nicholls, B. Henderson, B.H.T. Chai, *Opt. Mater.*, 6 (2001) 453.
- 19.K.C. Zhang, X.M. Wang, *Material Science for Nonlinear Optical Crystals*, Science Press, Beijing, 1996.
- 20.K.C. Zhang, L.H. Zhang, *Science and Technology for Crystal Growth*, Science Press, Beijing, 1997
- 21.T.M.Williams, D.Hunter, A.K.Pradhan, I.V.Kityk. *Appl. Phys. Lett.*, 89 (2006) 043116 .
- 22.J.Ebothe, I.V.Kityk, J.Kisilewski, T.Lukasiewicz, R.Diduszko, A.Majchrowski, *Appl.Phys.Lett.*, 89 (2006) 13110.